Soils and Foundations 2015;55(5):1001–1014

HOSTED BY

ELSEVIER

CrossMark

The Japanese Geotechnical Society

Soils and Foundations

www.sciencedirect.com

journal homepage: www.elsevier.com/locate/sandf

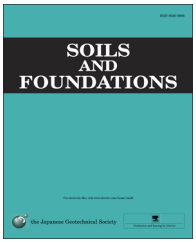

Bearing capacity analysis of open-ended piles considering the degree of soil plugging

Sangseom Jeong[a], Junyoung Ko[a,*], Jinoh Won[b], Kwangwoo Lee[a]

[a]*Department of Civil and Environmental Engineering, Yonsei University, 50 Yonsei-ro, Seodaemun-gu, Seoul 120-749, Republic of Korea*
[b]*Underground Engineering Team, Samsung C&T Corporation, 74 Seocho-daero, Seocho-gu, Seoul 137-956, Republic of Korea*

Received 18 April 2014; received in revised form 26 January 2015; accepted 15 March 2015
Available online 2 September 2015

Abstract

This paper presents a new design approach for predicting the degree of soil plugging and the inner skin friction of axial-loaded open-ended piles. The main objective of this study was to propose the SPT-based design method considering the plugging effect, since the SPT test is commonly used to identify the subsoil condition in sandy soils. The plugging effect for open-ended piles was quantified using field plugging measurements and the results of three full-scale field pile load tests. Based on the plugging measurements, the relationship of the plug length ratio (PLR) with the soil properties, pile geometry and pile driving condition was established. Additionally, a linear relationship between the PLR and incremental filling ratio (IFR) was proposed. Full-scale tests were performed on three instrumented piles with different diameters (508.0, 711.2 and 914.4 mm). An instrumented double-walled pile system was used to measure the outer and inner skin friction along the pile shaft. Based on the results of the full-scale field pile load tests, the inner skin friction of the open-ended piles was proposed as a function of the IFR and pile diameter. The predicted values were consistent with the measured values, such as the IFR and inner skin friction. The proposed method can predict the degree of soil plugging and the inner skin friction of open-ended piles and be selected as convenient option in engineering field.

Keywords: Plugging effect; Design method; Pile load test; PLR; IFR; Inner skin friction

1. Introduction

In recent years, open-ended steel pipe piles have been frequently used in the foundations of urban and coastal structures such as harbor terminals, long-span bridges and offshore wind power structures. Because an increasing number of massive structures are being constructed, it is becoming increasingly important to consider the plugging effect the application of open-ended steel pipe piles in foundation design. Some design methods for open-ended piles have been proposed. These methods have resulted in slightly different methodologies that can generally be classified into three groups: (1) cone-penetration test (CPT)-based design methods (Paik and Salgado, 2003; Yu and Yang, 2012; Kolk et al., 2005; Jardine et al., 2005; Lehane et al., 2005; Clausen et al., 2005) (2) standard penetration test (SPT)-based design methods (Lai et al., 2008), and (3) the earth pressure approach (API, 2007). However, the existing design methods have some limitations, such as a heavy dependence on the correlations that are derived from the model tests and CPTs. It is not easy to design the bearing capacity of open-ended piles considering the plugging effect in common practical cases, because the degree of plugging is not well reflected in the design methods. On the other hand, the main idea of this study is focused on

*Corresponding author.
E-mail address: jyko1225@yonsei.ac.kr (J. Ko).
Peer review under responsibility of The Japanese Geotechnical Society.

http://dx.doi.org/10.1016/j.sandf.2015.06.007

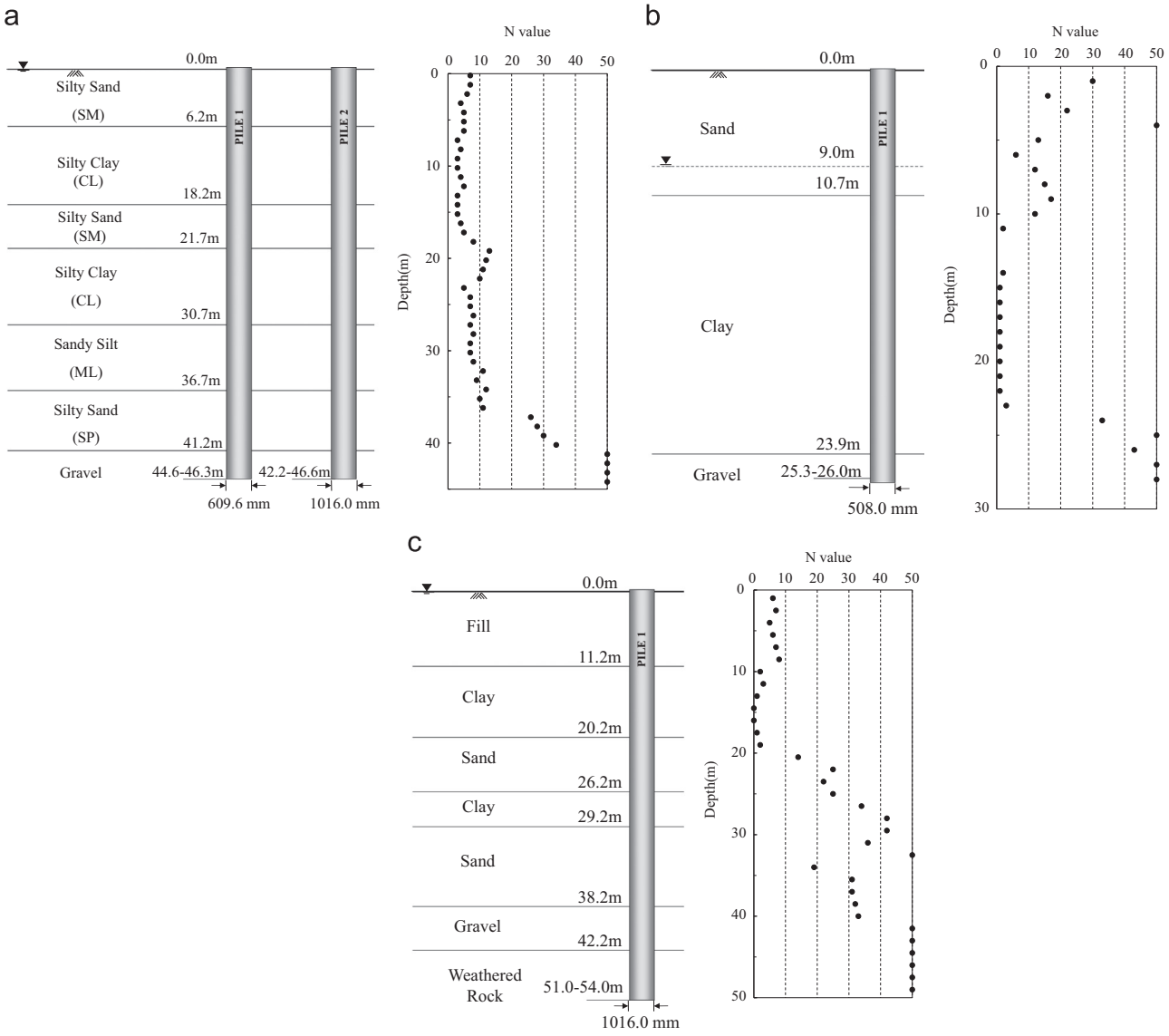

Fig. 1. Soil profile with the borehole and test piles for the PLR measurement. (a) Busan Nakdong river estuary weir site; (b) Busan Mieum district site; and (c) Incheon New Port site.

proposing the design method of driven piles in sands using SPT results. SPT test is common to identify subsoil condition especially in sandy soil. That is why the SPT-based method is selected as alternative one in engineering field.

The bearing capacity of open-ended piles is highly affected by the degree of soil plugging. Numerous studies have been conducted on the plugging effect of open-ended piles. Some researchers reported that the plugging effect of open-ended piles is highly influenced by the pile driving conditions (Brucy et al., 1991), pile geometry conditions (Beringen et al., 1979; Klos and Tejchman, 1981; Szechy, 1959; Kishida, 1967; Matsumoto and Takei, 1991), and soil conditions (Paik and Salgado, 2003). However, it is difficult to establish a distinct correlation between these factors and the plugging effect because of the complexity of the plugging effect.

The overall objective of this study is to propose an open-ended pile design methodology that considers the plugging effect using the results that are derived from full-scale tests and plugging measurements. Various influencing factors of the plugging effect should be quantified and considered when designing open-ended piles. The proposed methods were validated using a field case study. The predicted values, such as the incremental filling ratio (IFR) and inner skin friction are, compared with the measured values from the pile load tests. A new design methodology has been developed to provide a basis for a preliminary design method that would be applicable to open-ended piles taking into account the plugging effect.

2. Quantitative methods for the plugging effect on open-ended piles

The degree of soil plugging can be quantified using the plug length ratio (PLR) and IFR. The PLR is defined as the soil plug length per penetration depth at the end of the pile installation.

The PLR can be written as

$$\mathrm{PLR} = \frac{L_i}{D_p} \tag{1}$$

where L_i is the soil plug length and D_p is the penetration depth.

PLR = 0 represents that no soil enters the pile during pile installation. The behavior of open-ended piles in this condition is similar to the behavior of closed-ended piles. However, PLR = 1 represents that the soil plug length is equal to the pile penetration depth at the end of pile installation.

The IFR is defined as the increment of soil plug length per increment of pile penetration depth during pile installation. The IFR can be written as

$$\mathrm{IFR} = \frac{\Delta L_i}{\Delta D_p} \times 100(\%) \tag{2}$$

where ΔL_i is the increment of soil plug length and ΔD_p is the increment of penetration depth.

IFR = 0 and 1 are the fully plugged and fully unplugged conditions, respectively, and the IFR between 0 and 100 is the partially plugged condition.

The fully unplugged condition can be defined by using PLR which is greater than or equal to 1.0. However, the PLR can't be defined clearly for both the fully and partially plugged condition even though the IFR can be defined well for three different conditions of plugging (Paik, 1994). Therefore, it can be said that IFR is a better indicator of the degree of soil plugging than PLR (Paikowsky, 1989; Paik and Lee, 1993; Paik and Salgado, 2003). However, it is difficult to measure the IFR in engineering practice, whereas the PLR can be measured relatively easily. The approach to predicting the IFR from the PLR would be very convenience in the design stage. Therefore, it is necessary to investigate the relationship between the PLR and IFR.

3. PLR measurement

The plugging effect is highly complex and influenced by various factors. Previous studies on the plugging effect can be classified into three groups: (1) pile driving conditions, (2) pile geometry conditions and (3) soil conditions.

Brucy et al. (1991) reported that the soil plug length was increased when the driving energy was increased. Additionally, the soil plug length increased when the hammer weight was decreased and the height of fall was increased at constant energy. Then, the plugging effect decreases with increasing pile diameter (Beringen et al., 1979; Klos and Tejchman, 1981; Szechy, 1959) and decreasing pile length (Szechy, 1959; Kishida, 1967; Matsumoto and Takei, 1991).

Paik and Salgado (2003) performed model pile load tests using a calibration chamber. They reported that the IFR decreases with decreasing relative density and horizontal effective stress of soil, but is independent of the vertical effective stress of soil.

In this study, the PLR was measured on open-ended piles to investigate the plugging effect under various conditions such as pile driving conditions (hammer weight and height of fall), soil conditions (N value of the SPT result and horizontal effective stress) and pile conditions (pile length and pile diameter). The PLR measurement was conducted at the end of pile installation at three test sites in Korea: the Busan Nakdong river estuary weir site, Busan Mieum district site, and Incheon New port site. The pile diameters and penetration depths are 508–1016 mm and 26–45 m, respectively. Fig. 1 presents soil profiles with borehole and shaft embedment for the piles based on field test results.

Table 1
Geometries of the piles for PLR measurement.

Site	Number of piles	Pile diameters (mm)	Pile thickness (mm)	Pile length (m)
Busan Nakdong river	28	609.6	12	44.6–46.3
estuary weir site	24	1016.0	16	42.2–46.6
Busan Mieum district	66	508.0	12	25.3–26.0
site				
Incheon New port site	26	1016.0	16	51.0–54.0

The PLR values at the final penetration of 144 piles from the three different sites were obtained. The geometrical information of the piles for PLR measurements are presented in Table 1. The PLRs of 508 and 609 mm diameter piles are 0.60–0.85 and 0.71–0.89, respectively. The PLR range of the 1016 mm diameter piles is distributed above 0.90. These results demonstrate that the plugging effect of the open-ended piles decreases with an increase in the pile diameter. As previously mentioned, this result is consistent with the majority of studies by other researchers (e.g., Szechy, 1959; Kishida, 1967; Paikowsky, 1989).

To improve reliability of the proposed PLR equation, the formula should be non-dimensional. Therefore, the best reliable generalized form, with variables such as the pile diameter (D), pile penetration depth (L), hammer weight (W), height of the fall (h), SPT results (N) and horizontal effective stress of soil (σ_h'), was chosen to obtain the non-dimensional formula as shown in Eq. (3). The factors such as D^2/L and $\sigma_h'\sqrt{N}$ were obtained to separate the generalized form in terms of pile driving condition, pile condition and soil condition.

The correlations between the PLR and pile driving condition (E: driving energy), pile condition (D^2/L) and soil conditions ($\sigma_h'\sqrt{N}$) were plotted as shown in Fig. 2(a)–(c), respectively. As shown in Fig. 2(a), the measured range of driving energy between 50 kN m and 240 kN m for PLR lies in the typical range in the engineering field. This trend is the same as the results reported in the literature (Foray and Colliat, 2005; Paik et al., 2003; Reinhall and Dahl, 2011; Thandavamoorthy, 2004). Although the data distributions were scattered in Fig. 2, this is acceptable for engineering applications, considering that the coefficient of determination (R^2) of plugging effect prediction for field data is typically low (Yu and Yang, 2012; Japan Road Association (JRA), 2006; Architectural Institute of Japan (AIJ), 2004). The PLR is linearly correlated with the influencing factors. To obtain the best regressions, the empirical method for the PLR can be proposed using the analysis of the PLR measurement.

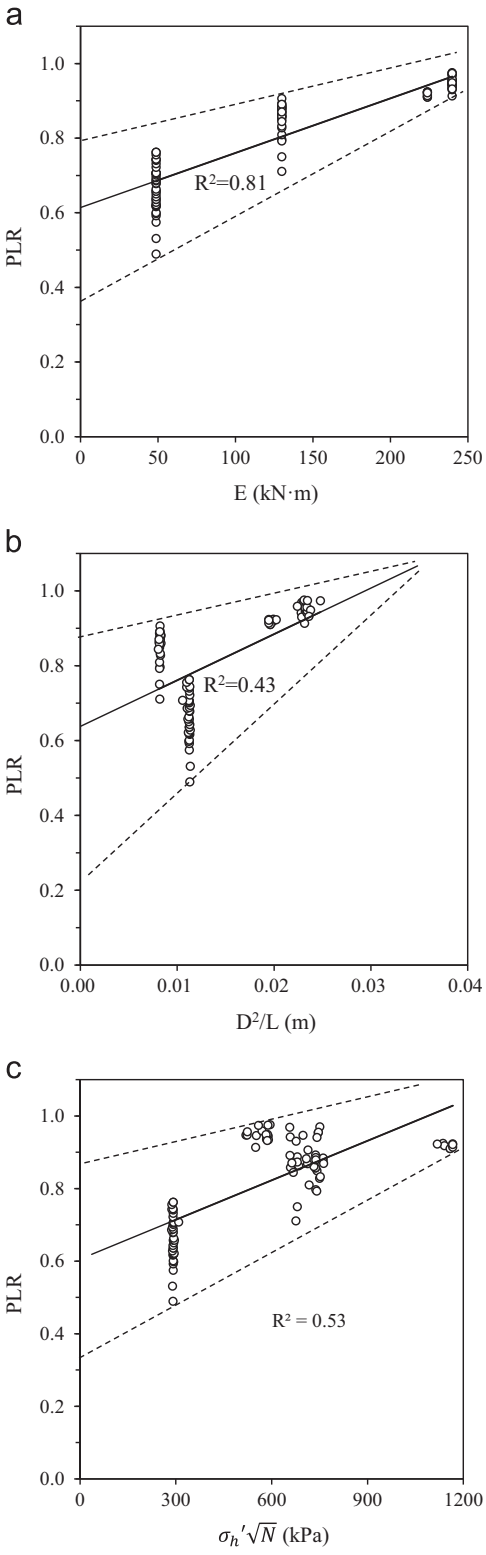

Fig. 2. Correlations between the PLR and influencing factors. (a) variation of PLR with driven energy; (b) variation of PLR with pile geometry condition (D^2/L); and (c) variation of PLR with soil condition ($\sigma h'\sqrt{N}$).

4. Proposed PLR prediction methods

There are few PLR prediction methods for open-ended piles. The existing design methods (Paik and Salgado, 2003; Yu and Yang, 2012; Kolk et al., 2005; Jardine et al., 2005; Lehane et al., 2005; Clausen et al., 2005) rely on highly the CPT results. On the other hand, because SPT test is common to identify subsoil condition in sandy soil, the SPT-based method is selected as alternative one in engineering field. However, a few SPT-based methods (Lai et al., 2008) are proposed. Therefore, an appropriate PLR prediction method is necessary for a rational design in the preliminary design stage.

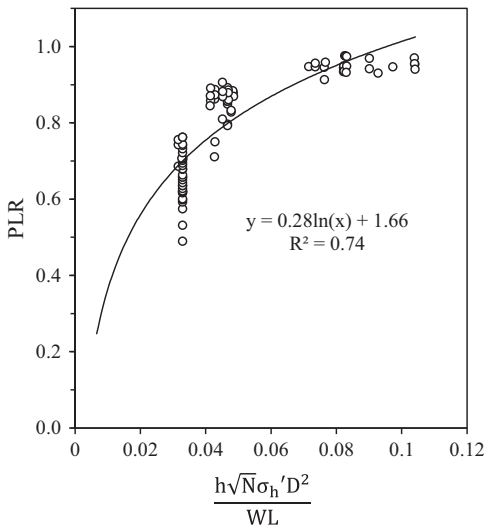

Fig. 3. Proposed PLR equation.

PLR measurement data from 144 field cases are analyzed under various conditions. The results of the PLR measurements, indicate that the PLR depends on the pile driving condition (E: driving energy), pile condition (D^2/L) and soil conditions ($\sigma'_h\sqrt{N}$). Therefore, based on the aforementioned correlations between the PLR and the influencing factors, the generalized function of the PLR is modified to consider the plugging effect by introducing Eq. (3). Both the PLR and the generalized form are non-dimensional.

$$\mathrm{PLR} = a\ln\left(\frac{h\sqrt{N}\sigma'_h D^2}{WL}\right) + b \quad \left(\text{for } \frac{h\sqrt{N}\sigma'_h D^2}{WL} \geq 0.04\right) \tag{3}$$

where N is the value of the SPT, σ'_h is the horizontal effective stress of soil (kPa), D is the pile diameter (m), h is the height of the fall (m), L is the pile penetration depth (m), W is the hammer weight (kN), and a and b are the fitting parameters. Eq. (3) can be applied for values in x-axis greater than 0.4.

Regression analysis is used to obtain the best-fit values of a and b. Fig. 3 presents the variation of the PLR against the generalized form based on the results obtained in a total of 144 PLR measurements. From the regression analysis, parameters a and b are determined to be 0.28 and 1.66, respectively. Through the regression analysis, the empirical Eq. (4) for the PLR can be rewritten as follows:

$$\mathrm{PLR} = 0.28\ln\left(\frac{h\sqrt{N}\sigma'_h D^2}{WL}\right) + 1.66 \tag{4}$$

If the PLR is not available from direct measurements, the proposed PLR prediction method can predict the soil plug length in the preliminary design stage.

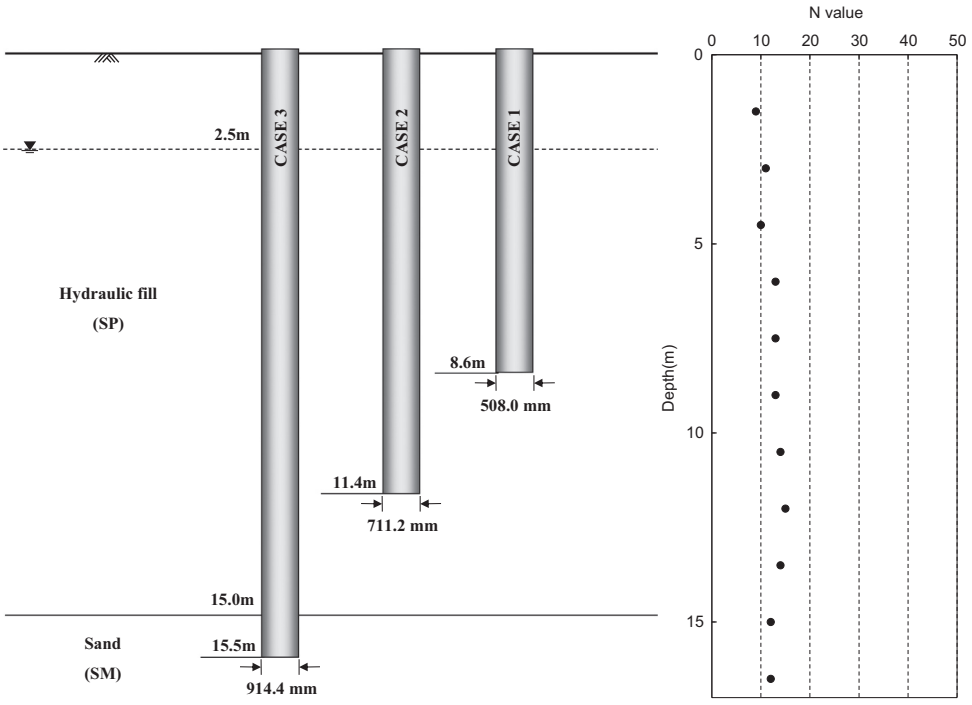

Fig. 4. Soil profile with the borehole and embedment for test piles (Kwangyang site).

5. IFR measurement and field pile load test

IFR measurement and field pile load tests were conducted on full scale piles instrumented with strain gauges to investigate the relation between the plugging effect and bearing capacity. The emphasis was on analyzing the plugging effect from the soil plug in the pile so that these tests were performed on 3 test piles under various conditions, such as pile diameter and pile length.

5.1. Site and subsurface description

The test site was located at the Kwangyang substiuted natural gas (SNG) plant in Korea. A geotechnical investigation was performed to define the soil profile and properties at the test site as accurately as possible. The in-situ field testing was performed on two boring holes (BH-1 and BH-2) with conventional sampling near the test piles and standard penetration testing (SPT). Fig. 4 presents the soil profile with borehole and schematic representation of the instrumented piles.

The soil obtained by the boring and lab tests, is generally composed of a thick hydraulic fill layer with sand. The results of SPTs indicate that sand deposits at 0 to 15 m were in a loose state with SPT N values ranging from 8 to 18. The water table was located at 2.5 m below the ground surface. The cohesionless soils were classified as SP or SM with round angularity according to the Unified Soil Classification System (ASTM, 2011). The properties of soils based on the site investigation are summarized in Table 2.

Table 2
Physical properties of in-situ soil.

Soil	Hydraulic fill	Sand
Total unit weight, γ_t (kN/m^3)	17.6	18.0
Poisson's ratio, μ_s	0.3	0.3
Friction angle (°)	32	33
N value	8–18	12–27

5.2. Installation of the test piles

Full-scale field load tests were performed on three instrumented piles to investigate the relation between the plugging effect and bearing capacity.

The bearing capacity of open-ended piles consists of three components: the outer skin friction, annulus load capacity, and inner skin friction (or soil plug capacity). The instrumented double-walled pile system (Paik et al., 2003) can be applied to separate all resistance components of the open-ended piles. A schematic representation of the instrumented piles is shown in Fig. 5. The instrumented piles, TP-1, TP-2, and TP-3, have outer diameters of 508.0, 711.2, and 914.4 mm, respectively. The instrumented piles were prefabricated in factories. The gap between the outer and inner piles was welded to prevent any soil intrusion during the installation and testing. Each pile was driven by a hydraulic hammer, DKH-13 (hammer weight: 130 kN, max potential energy: 156 kN · m). To prevent potential damage due to strain gauges during pile driving, the free fall height of the hammer was 0.3 m. The final penetration depths of TP-1, TP-2 and TP-3 were recorded as 8.6, 11.4, and 15.5 m, respectively.

Automated equipment including linear variable differential transformers (LVDTs) and strain gauges were used. Two LVDTs were installed on the pile head to measure the settlement with sequential loading steps, and 32 strain gauges (electrical resistance type: 20, vibration wire type: 12) per instrumented pile were installed around the pile circumference every 90° to

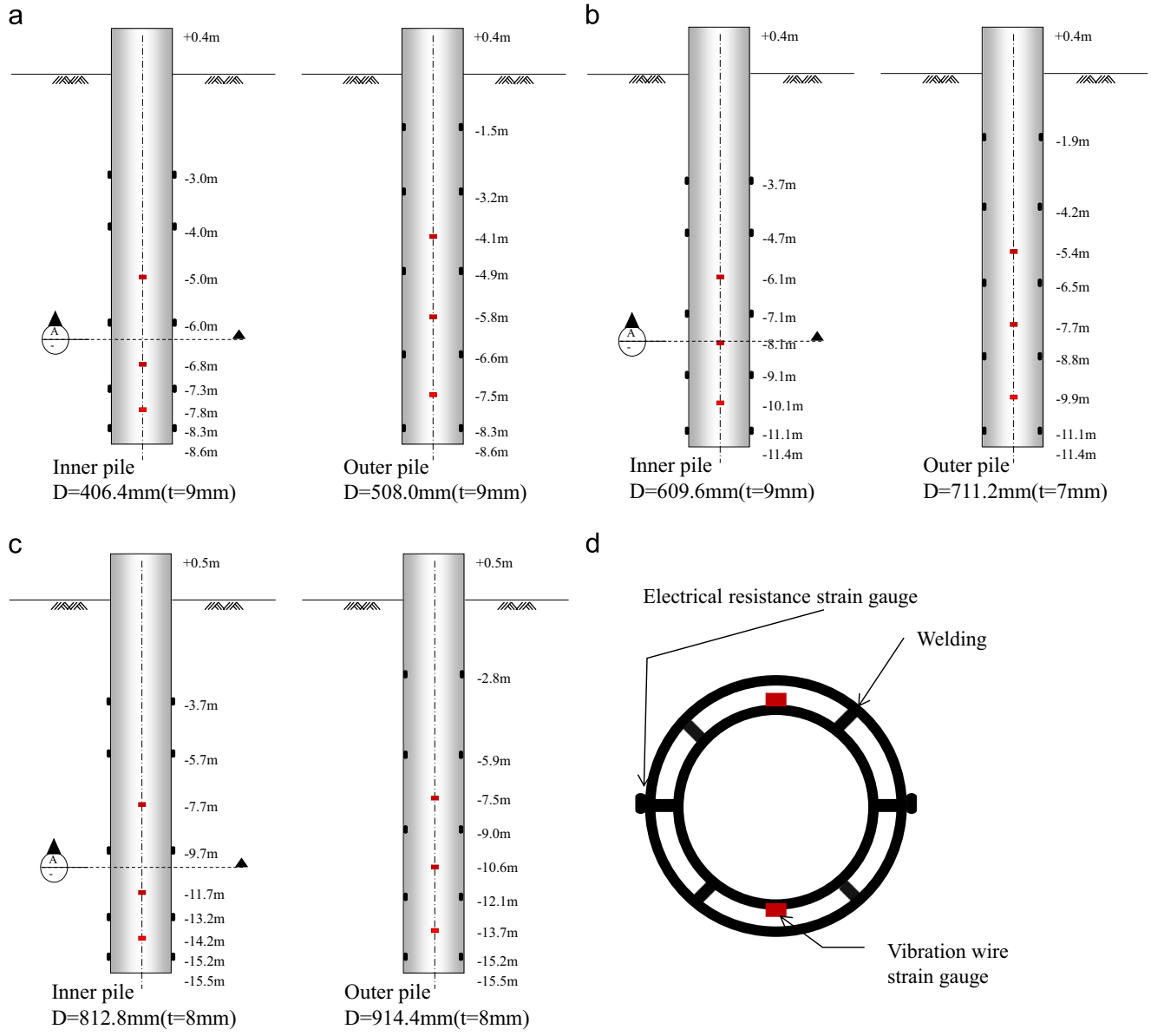

Fig. 5. A schematic representation of instrumented piles. (a) TP-1 (outer diameter=508.0mm); (b) TP-2 (outer diameter=711.2mm); (c) TP-3 (outer diameter=914.4mm); and (d) sectional view of instrumented piles.

measure all components of the bearing capacity for the open-ended piles. These gauges were sealed with a thin membrane to prevent mechanical damage. The output from the LVDTs and strain gauges was acquired using a 200-channel carrier frequency amplifier and computer data-acquisition system.

Fig. 6 shows the penetration depth versus the penetration depth per blow. The penetration per blow for TP-1 was greater than TP-2 and TP-3 until a penetration depth of 4.5 m. After 4.5 m, the penetration per blow for TP-1 was very similar to TP-2 and TP-3.

All test piles were initially set in unplugged conditions. As the pile driving continued, inner shaft resistance mobilized between the soil plug and the inner piles, depending on the degree of soil plugging. Because of the differences in the magnitude of mobilizing inner shaft resistance, the penetration per blow for TP-1 was initially greater than the others. The penetration per blow for TP-1 was suddenly decreased, but the penetration per blow for TP-2 and TP-3 were varied slightly. This result shows that the soil plugging of TP-1 was developed higher than that of TP-2 and TP-3, clearly indicating that the degree of soil plugging depends on the diameter of the pile diameter.

5.3. IFR measurement

The degree of soil plugging in the open-ended piles affects the pile behavior. The IFR is a good indicator of the degree of soil plugging (Paik and Salgado, 2003). The IFR is defined as the increment of soil plug length per increment of pile penetration depth during pile installation (see Eq. (2)). The increment of penetration depth (ΔD_p) was assumed as 1.0 m. During the pile driving, the IFR was measured at each increment of 1.0 m penetration depth. Fig. 7(a) presents the relationship between the measured soil plug length L_i and pile penetration depth D_p. The soil plug length increased almost linearly with the penetration depth, but all test piles were not in the unplugged state. The soil

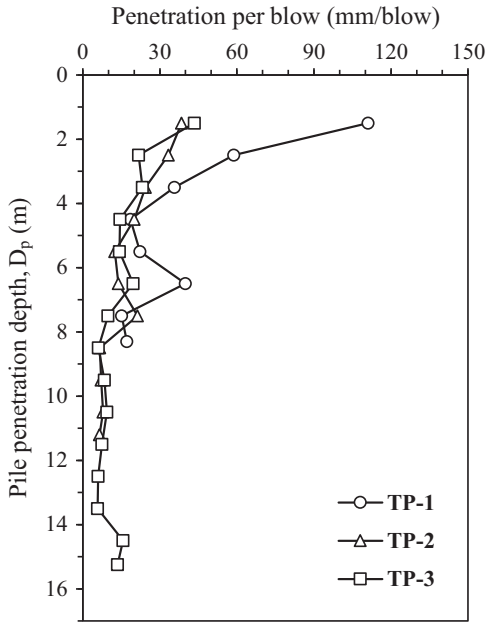

Fig. 6. Penetration per blow with depth.

plug length increased with the pile penetration depth, and with increasing the pile diameters at the same penetration depth.

In Fig. 7(b), the results from Ko and Jeong (2015) were obtained from the comparison with the IFR and *N* value. The inner skin friction between the soil plug and the inner piles varied, depending on the degree of soil plugging. Because of the difference in magnitude of the mobilized inner skin friction, TP-1 had a smaller IFR than the others test piles. Additionally, the IFR of all test piles had consistent trends. For all test piles, the IFR significantly decreased with the penetration depth from 0–2.5 m to 6–7.5 m and increased with the penetration depth from 2.5–6 m to 7.5–9 m. This results show that the IFR increases with an increase of *N*, and vice versa. It is evident that the soil condition and pile diameter are highly correlated with the IFR.

5.4. Field load test

Full-scale tests, including dynamic and static axial-compression load tests, were performed on the three instrumented piles with different diameters (508.0, 711.2 and 914.4 mm). To measure the outer and inner skin friction that acted on the piles, a double-walled system was used with instrumented strain gauges on the outside and inside walls of the pile. Dynamic load tests were performed to evaluate the bearing capacity of the piles at the end of initial driving (EOID) following the ASTM D4945 protocol (ASTM, 2013b). The Case Pile Wave Analysis Program (CAPWAP) indicated that the ultimate bearing capacities of TP-1, TP-2 and TP-3 were 1031, 2240 and 3100 kN at EOID, respectively.

Due to the site conditions, static axial-load tests were performed 45 days after the EOID to investigate the setup effect. The static load tests were conducted in compression based on the ASTM D1143 protocol (ASTM, 2013a). Twelve earth anchors were installed at the test site to serve as a reaction. A schematic representation of the loading system for

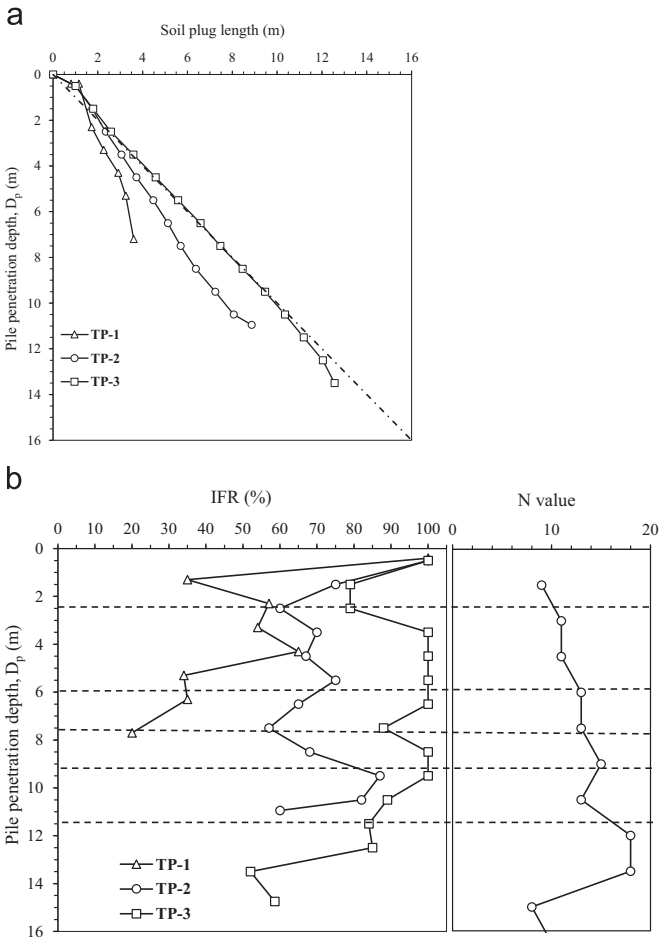

Fig. 7. Result of IFR measurements, pile penetration depth versus: (a) soil plug length; (b) IFR.

the static load test is provided in Fig. 8. The maximum loads applied were 250% of the design loads. The loading and unloading were systematically performed in 5 cycles and 10 steps. During the loading stage, each step lasted a minimum of 20 min, whereas the step duration was no less than 10 min during the unloading stage.

The axial-load distribution profiles are obtained by analyzing the measured strain gauge data along the pile inside and outside. The typical test results are presented in Figs. 9 and 10 in terms of the penetration depth versus the axial-load distribution and the load-settlement curves, respectively. As shown in Fig. 10, the ultimate bearing capacities of piles TP-1, TP-2, and TP-3 were 1000, 2000 and 3000 kN, respectively. As shown in Fig. 9 (a), (c) and (e), it is shown that inner skin friction was mobilized within a distance of 1.3–2.3 m from the pile tip. It was found that the soil plug in the lower part considerably influenced on the inner skin friction. This trend is generally consistent with previous studies (Paikowsky, 1990; Yu and Yang, 2012).

6. Proposed relationship between the PLR and IFR

The PLR was measured at the end of pile driving, but the IFR was measured during the pile installation. Therefore, it is easier to obtain the PLR than the IFR in the design stage. In most previous studies, the IFR is considered proportional to

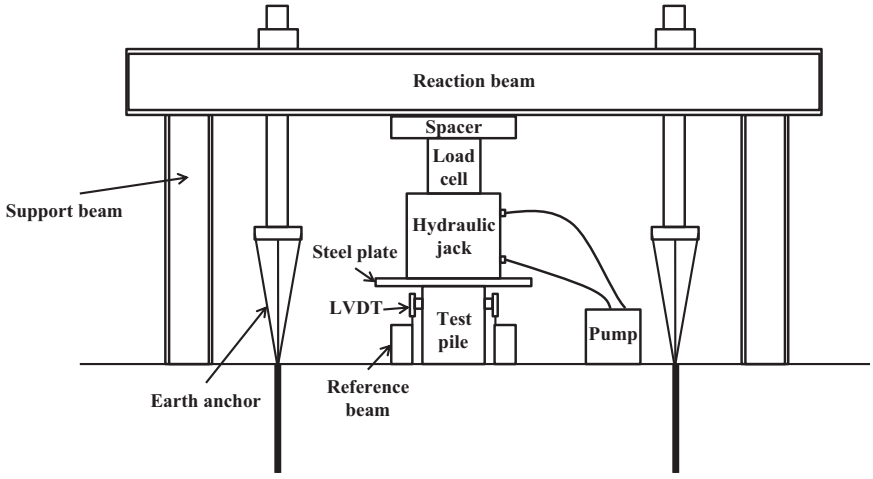

Fig. 8. A schematic representation of loading system for static load test.

the PLR (Paik et al., 2003). To investigate the relationship between the PLR and IFR, it is necessary to analyze the results of the PLR and IFR field measurements.

The PLR and IFR measurement data from three field cases were analyzed. Based on the aforementioned previous studies, a trend line for the test data can be proposed in the form of

$$\mathrm{IFR} = a(\mathrm{PLR}) + b \tag{5}$$

where PLR is the plugging length ratio, and a and b are the fitting parameters.

Fig. 11(a) presents the relationship between the PLR and IFR based on the results obtained from the field tests reported in this manuscript. From the linear regression analysis, the parameters a and b were determined to be 110.3 and −11.5, respectively, and the following empirical equation for the relationship between the PLR and IFR can be written as follows

$$\mathrm{IFR} = 110.3(\mathrm{PLR}) - 11.5 \tag{6}$$

In previous studies, Paik and Salgado (2003) reported the relationship between the PLR and IFR, which can be expressed as follows for the calibration chamber tests:

$$\mathrm{IFR} = 109(\mathrm{PLR}) - 22 \tag{7}$$

The fully unplugged condition can be determined by using PLR which is greater than or equal to 1.0 (Paik, 1994). As shown in Fig. 11(b), two points of PLR higher than 1 were in the fully unplugged condition. Fig. 11(b) compares this study and other studies. Eq. (6) slightly overestimates the IFR for Eq. (7). In addition, Eq. (6) generally overestimates the IFR given by PLR values lower than 0.85, as shown in Fig. 11(b). It is shown that there is a difference in the trend between this study and the existing method because the pile diameter (D) of this study is larger (508.0–914.4 mm) than the other field cases (D=356.0 mm) or model cases. Therefore, the proposed relationship between the PLR and IFR given by Eq. (6) was notably realistic and convenient for the preliminary design stage of open-ended piles.

7. Proposed equation of the inner skin friction

7.1. Influence zone of the inner skin friction

The inner skin friction occurs mainly along the lower part of the soil plug because the soil arching is significant and a large lateral coefficient of earth pressure is achieved (Paikowsky, 1990; Yu and Yang, 2012; Liu et al., 2012). Therefore, it is necessary to accurately predict the influence zone of inner skin friction.

The influence zone of the inner skin friction can be quantified by measuring the axial-load distributions of the inner piles. As previously mentioned, the results of the static axial-load tests indicate that most of the inner skin friction was occurred within a distance of 1.3–2.3 m from the tip at the ultimate loading state, as shown in Fig. 9(a), (c) and (e). This topic can be investigated further by analyzing the soil plugging index (SPI) with respect to the pile inner diameter. The soil plugging index (SPI) is defined as

$$\mathrm{SPI} = \frac{L_{is}}{L_i} \times 100 \tag{8}$$

where L_i is the soil plug length and L_{is} is the length of the developing inner skin friction. The SPI that was calculated in Paik et al. (2003) is also plotted for comparison. Fig. 12 illustrates the variation of the SPI with the pile inner diameter. The inner skin friction was largely developed near the pile tip at 18–34% of the total soil plug length. Furthermore, the SPI linearly decreased with increases in the pile inner diameter, which indicates that the soil plugging in the lower portion considerably influences the inner skin friction. The soil plugging index (SPI) based on the combined test results is expressed as

$$\mathrm{SPI} = -0.03D_i + 43.2 \tag{9}$$

where D_i is the inner pile diameter (mm).

7.2. Inner skin friction

Since the 1990s, the one-dimensional plug analysis has been modified to increase in its accuracy (Murff et al., 1990; O'Neill

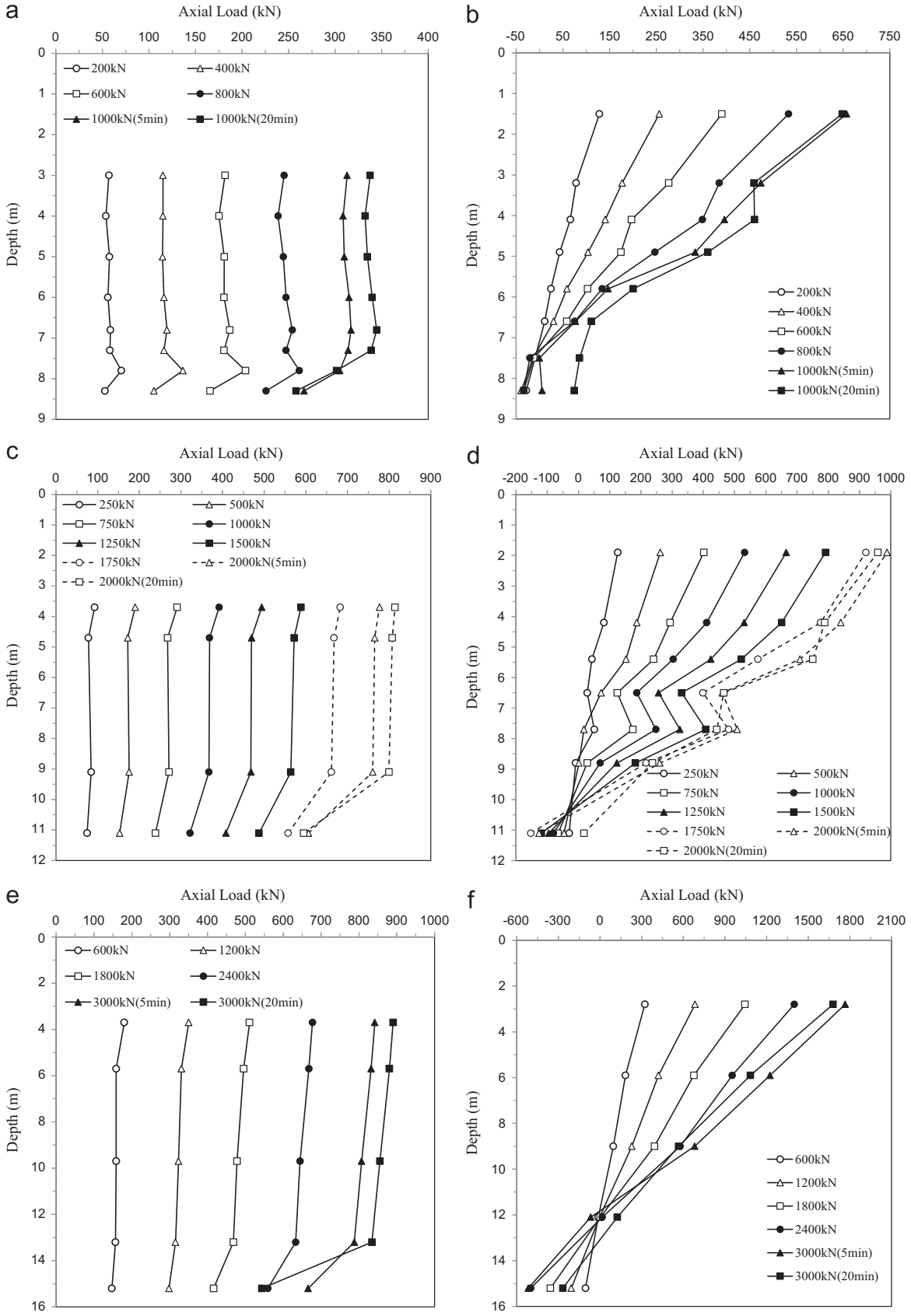

Fig. 9. Axial load distributions of inner and outer pile. (a) inner pile of TP-1; (b) outer pile of TP-1; (c) inner pile of TP-2; (d) outer pile of TP-2; (e) inner pile of TP-3; and (f) outer pile of TP-3.

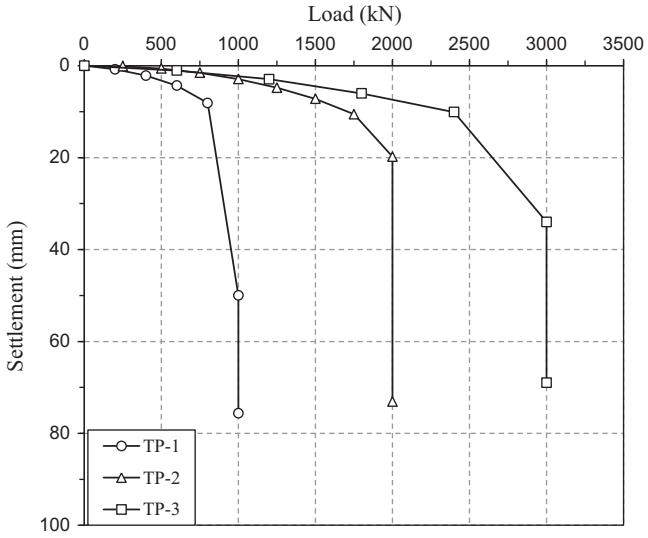

Fig. 10. Load-settlement curve.

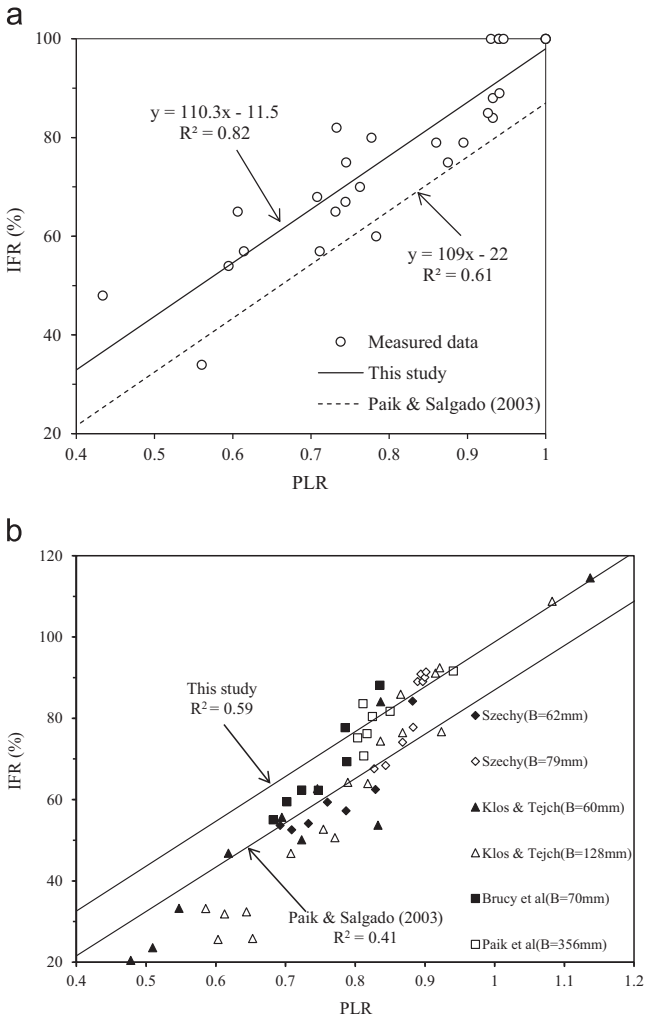

Fig. 11. The relationship between the PLR and IFR.

and Raines, 1991; Randolph et al., 1991). Randolph et al. (1991) reported the equilibrium equation for the one-dimensional plug analysis shown in Fig. 13. Lehane and

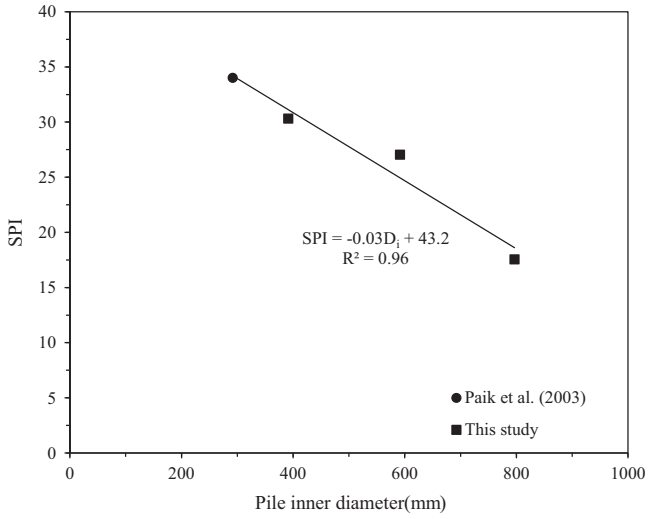

Fig. 12. Variation of SPI with pile inner diameter.

Gavin (2001) later reported that it was reasonable to assume that the shear stresses, which could develop at any location on the inner pile wall, were directly proportional to the vertical effective stress at that level.

Because of the fast rate of excess pore water pressure dissipation, the drained condition is assumed for sand with piles driven into it, and drained parameters are used in the analysis. The unit average skin friction can be calculated from the following Eq. (10) based on the analysis of effective stress.

$$f_s = K_0\sigma_v' \tan\delta = \beta\sigma_v' \tag{10}$$

where K_0 is the Rankine earth pressure coefficient, σ_v' is the effective vertical stress and δ is the angle of interface friction between the soil and inner pile wall. A simple analytical treatment of the soil plug response under drained conditions has been presented by Randolph (1988).

This method is sensible and not overly conservative. In addition, because this method can be applied without CPT results, it is extremely useful in the preliminary design stage. However, the existing method did not consider the plugging effect.

The main objective in this research is to discover the relation between the inner skin friction and both the IFR and pile diameter. However, because there were limited data on the inner skin friction, other existing tests were used for the proposed equation of the inner skin friction. To investigate the relationship, three sets of tests are applied and analyzed. Table 3 summarizes the descriptions of the three sets.

The unit inner skin friction f_{si}, which was normalized with respect to $K_0\sigma_v'\tan\delta$, is plotted versus (IFR · D) in Fig. 14. A trend line for the test data in Fig. 14 is proposed in the form

$$\frac{f_{si}}{K_0\sigma_v' \tan\delta} = a(\mathrm{IFR}\times D)^b \tag{11}$$

where f_{si} is the unit inner skin friction (kPa), K_0 is the Rankine earth pressure coefficient before pile driving, σ_v' is the average vertical effective stress over the entire penetration depth (kPa), δ is the angle of interface friction between the soil and inner pile wall (°), and D is the pile diameter (m). Through regression analysis, parameters a and b are determined as

33.4 and −0.48, respectively, and Eq. (11) is rewritten as

$$\frac{f_{si}}{K_0\sigma_v' \tan\delta} = 33.4(\mathrm{IFR}\times D)^{-0.48} \quad (12)$$

The proposed equation of the inner skin friction can predict the bearing capacity considering the degree of soil plugging in the preliminary design stage.

The inner skin friction occurs nearby the pile tip. The influence zone of the inner skin friction can be quantified by the axial-load distribution of inner piles. The proposed SPI is a function of the inner pile diameter. The length of mobilizing inner skin friction is obtained as follows.

$$L_{is} = \frac{L_i \times \mathrm{SPI}}{100} \quad (13)$$

The actually mobilizing inner skin friction can be obtained by using the obtained L_{is}.

$$Q_{si} = f_{si} \times A_{si} = f_{si} \times \pi D_i L_{is} \quad (14)$$

where Q_{si} is the actually mobilizing inner skin friction, f_{si} is the unit inner skin friction, A_{si} is the area of the mobilizing inner skin friction and D_i is the inner pile diameter.

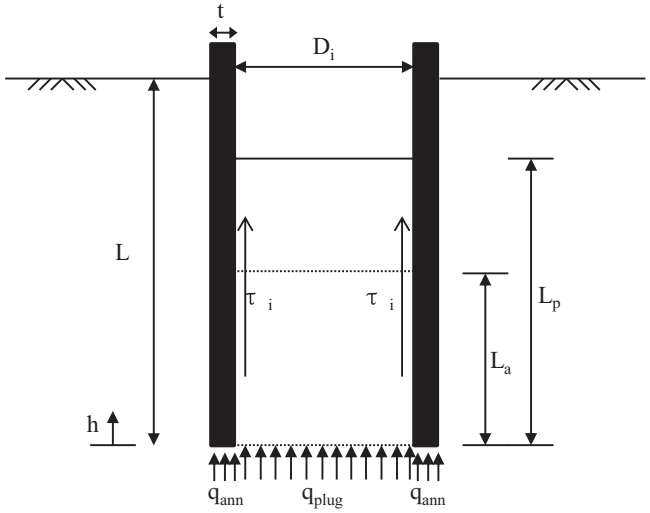

Fig. 13. Equilibrium of soil plug (Randolph et al. 1991).

8. Validation of the proposed design method

8.1. Validation of the relationship between the PLR and IFR

In this section, the validation of the relationship between the PLR and IFR is discussed. The proposed relationship between the PLR and IFR was validated by comparing the results from the Paik and Salgado method (see Eq. (7)) with some of the measured results in details in Table 4. Twelve measured results are collected as the representative large-diameter piles, which have diameters of 0.763 m to 2 m. Fig. 15 compares the performance of the proposed method with the other method. The proposed method can predict the IFR more accurately than the existing method.

8.2. Comparison with case history (Paik et al, 2003)

The proposed method was validated by comparison with the field-measured results. The pile and soil properties for the case history were the same properties mentioned in the reference. Also, the values for the measured data such as the IFR, the influence zone of the inner skin friction, and the inner skin friction were the same as those in the reference.

The IFR, the influence zone of the inner skin friction and the inner skin friction of the test pile (open-ended pile), which was installed in sand at Lagrange County in Indiana (Paik et al.,

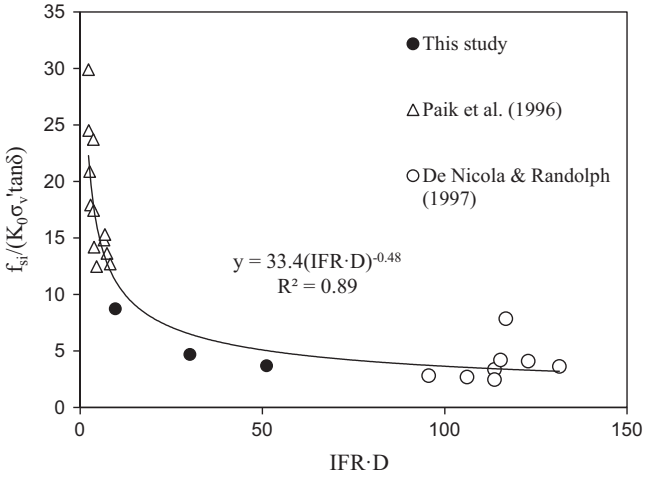

Fig. 14. Proposed equation for inner skin friction.

Table 3
Description of test results for analysis of inner skin friction.

Reference	Description
Paik et al. (1996)	Pile geometry: L=0.908 m, D=42.7–89.1 mm, and d=36.5–74.2 mm Soil property: sand; D_r=55 and 90% Test method: Calibrated chamber tests
De Nicola and Randolph (1997)	Pile geometry: L=5.2–16.7 m, D=1.6 m, and d=1.49 m in prototype Soil property: silica flour; D_r=68, 85, and 95% Test method: centrifuge chamber tests
This study	Pile geometry: L=8.6–15.5 m, D=0.508–0.914 m, and d=0.3884–0.8984 m in full-scale pile Soil property: sand, silty sand Test method: full-scale tests

2003), were compared with the predicted values by the proposed design method. Fig. 16 presents a soil profile and the shaft embedment for a test pile: Test pile (open-ended pile), which was 356 mm in diameter and 8.24 m long. In addition, Paik et al. (2003) reported that the angle of interface friction between the soil and inner pile wall δ is 22.2°; K_0 is 0.55; σ_v' is 101.2 kPa; and PLR is 0.82.

Table 4
Details of measured PLR and IFR values.

Case	Reference	D (m)	PLR	IFR (%)
C1	Jardine et al. (2005)	0.76	1.00	89
C2	Kikuchi et al. (2007)	1.50	1.00	100
C3		1.50	1.00	100
C4	Ishihara et al. (1977)	1.20	0.77	77
C5	Shioi et al. (1992)	2.00	1.08	100
C6	Kusakabe et al. (1989)	0.80	1.00	100
C7		1.20	0.85	85
C8	Pump et al. (1998)	0.91	0.80	85
C9		0.91	0.85	80
C10	Fugro Engineers (1995)	0.76	1.00	100
C11	Fugro Engineers (2004)	0.76	1.00	100
C12		0.76	1.00	100

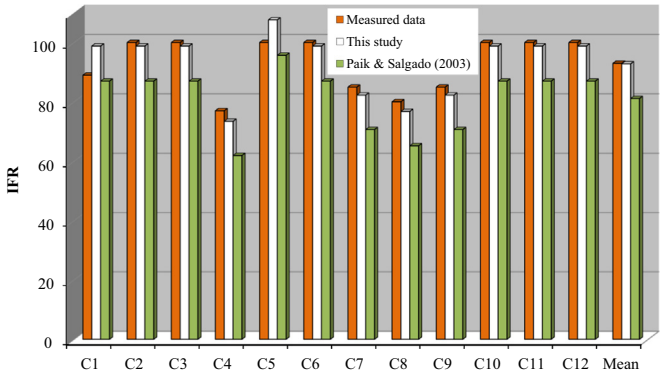

Fig. 15. Comparison with other method for relationship between the PLR and IFR.

The IFR can be predicted using Eq. (6) as follows:

$$\mathrm{IFR} = 110.3(\mathrm{PLR}) - 11.5 = 110.3(0.82) - 11.5 = 78.9$$

The SPI can be predicted using Eq. (9) as follows:

$$\mathrm{SPI} = -0.03D_i + 43.2 = -0.03(292) + 43.2 = 34.44$$

$$\mathrm{SPI} = \frac{L_{is}}{L_i} \times 100 = 34.44$$

The obtained influence zone of the inner skin friction is

$$L_i = \mathrm{PLR} \times D_i = 0.82 \times 7.04 = 5.77\ m$$

$$L_{is} = \frac{34.44 \times L_i}{100} = \frac{34.44 \times 5.77}{100} = 1.99\ m$$

The inner skin friction can be computed using Eq. (12). The calculation is summarized as follows:

$$\frac{f_{si}}{K_0\sigma_v' \tan\delta} = 33.4(\mathrm{IFR} \times D)^{-0.48}$$

$$f_{si} = 33.4(\mathrm{IFR} \times D)^{-0.48} \times K_0\sigma_v'$$

$$\tan\delta = 33.4(78.9 \times 0.292)^{-0.48} \times (0.55)(101.2)(\tan 22.2) = 168.3\ \mathrm{kPa}$$

$$Q_{si} = f_{si} \times A_{si} = f_{si} \times \pi D_i L_{is} = 168.3 \times \pi(0.292)(1.99) = 307.2\ \mathrm{kN}$$

The predicted IFR, the influence zone of the inner skin friction, and the inner skin friction were 101.8, 97.5, and 91.4%, respectively, of the values determined from the field measurements on pile OEP.

9. Summary and conclusions

The primary objective of this study was to propose a new empirical method to quantify the bearing capacity and soil

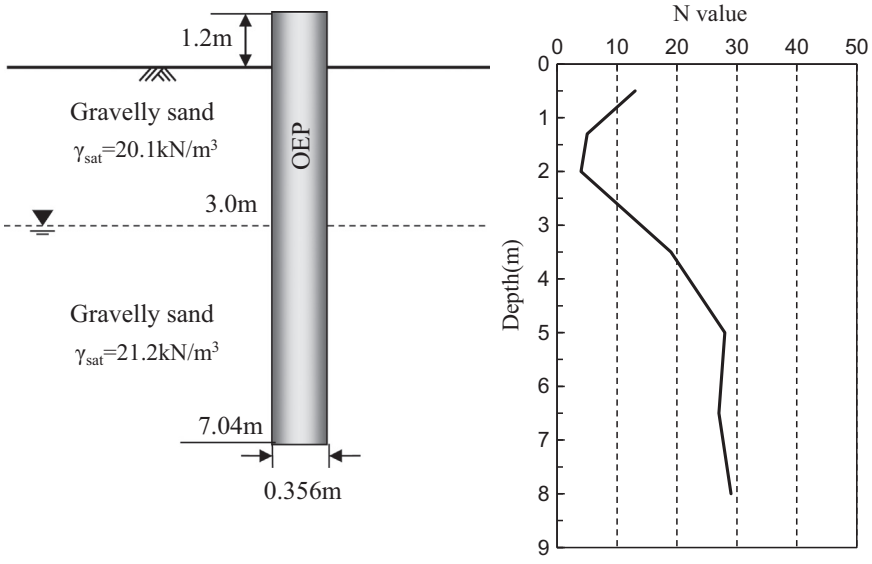

Fig. 16. Test pile and soil condition of Paik et al. (2003).

plugging (PLR, IFR) for open-ended piles. A series of field load tests and plugging measurements were conducted to investigate the plugging effect. Static axial-compression load tests were performed on three instrumented piles with different diameters (508.0, 711.2, and 914.4 mm). Direct observations on the soil plugs were made and used to quantify the PLR and IFR. Additionally, a regression analysis was conducted to determine the PLR, IFR, and inner skin friction equations. Compared to the case history, the proposed method was consistent with the in-situ measurements. The following conclusions can be drawn based on the findings of this study:

1. The proposed PLR and IFR equations can predict the degree of soil plugging in the preliminary design stage. In the field, it is easier to measure the PLR than the IFR. The proposed IFR equation can be used based on the PLR when only the PLR is measured in the field.
2. The IFR is a good indicator of the degree of soil plugging. Therefore, by accounting for the IFR, the proposed inner skin friction equation is an appropriate and realistic representation of the plugging effect characteristics.
3. Compared with the results of the case history, the proposed method, which uses the PLR, IFR and, inner skin friction, can accurately predict the degree of soil plugging of open-ended piles. The proposed design method, which consider the degree of soil plugging, can overcome the limitations of the existing design methods

Nomenclature

The following symbols are used in this paper:

a	fitting parameter
A_{si}	area of the mobilizing inner skin friction
b	fitting parameter
D	pile diameter
D_i	inner pile diameter
D_p	penetration depth
E	driving energy
f_s	unit skin friction
f_{si}	unit inner skin friction
h	height of the fall
K_0	Rankine earth pressure coefficient
L	pile penetration depth
L_i	soil plug length
L_{is}	length of the developing inner skin friction
N	value of the SPT
Q_{si}	actually mobilizing inner skin friction
W	hammer weight
ΔD_p	increment of penetration depth
ΔL_i	increment of soil plug length
σ_h'	horizontal effective stress of soil
σ_v'	vertical effective stress of soil
δ	angle of interface friction

Acknowledgements

This work was supported by the National Research Foundation of Korea (NRF) grant funded by the Korea government (MSIP) (no. 2011-0030040).

References

API, 2007. Recommended Practice for Planning, Designing and Constructing Fixed Offshore Platforms-working Stress Design, 21st ed. American Petroleum Institute, Dallas, TX.

ASTM, 2011. Standard Practice for Classification of Soils for Engineering Purpose (Unified Soil Classification System). D2487, West Conshohocken, PA.

ASTM, 2013a. Standard Test Methods for Deep Foundations Under Static Axial Compressive load. D1143, West Conshohocken, PA.

ASTM, 2013b. Standard Test Method for High-strain Dynamic Testing of Piles. D 4945, West Conshohocken, PA.

Architectural Institute of Japan (AIJ), 2004. Recommendations for Design of Building Foundations. Architectural Institute of Japan, Tokyo.

Beringen, F.L., Windle, D., Van Hooydonk, W.R., 1979. Results of loadings tests on driven piles in sand. In: Proceedings of International Conference of the Institution of Civil Engineers on Recent Developments in the Design and Construction of Piles, London, pp. 213–225.

Brucy, F., Meunier, J., Nauroy, J. F., 1991. Behavior of pile plug in sandy soils during and after driving. In: Proceedings of 23rd Annual Offshore Technology Conference, Houston, 1, pp. 145–154.

Clausen, C.J.F., Aas, P.M., Karlsrud, K., 2005. Bearing capacity of driven piles in sand, the NGI approach. In: Proceedings of the International Symposium on Frontiers in Offshore Geotechnics, Taylor & Francis, London, pp. 677–681.

De Nicola, A., Randolph, M.F., 1997. The plugging behavior of driven and jacked piles in sand. Geotechnique 47 (4), 841–856.

Foray, P. Y., Colliat J. –L., 2005. CPT-based design method for steel pipe piles driven in very dense silica sands compared to the Euripides pile load test results. In: Proceedings of the International Symposium on Frontiers in Offshore Geotechnics, Taylor & Francis, London, pp. 669–675.

Fugro Engineers B.V., 1995. Interpretation Report on Reduced Scale Pile Load Tests. Report no. K-2380/207. Jamuna Bridge, Bangladesh.

Fugro Engineers B.V., 2004. Axial Pile Design Method for Offshore Driven Piles in Sand. Report no. P-1003, Issue 3 to API, 5, pp. 122.

Ishihara K., Saito A, Shimmi Y., Mieura Y., Tominaga M., 1977. Blast furnace foundations in Japan. In: Proceedings of the Ninth International Conference on Soil Mechanics and Foundation Engineering, Tokyo, pp. 157–236.

Japan Road Association (JRA), 2006. Specifications for Highway Bridges, Part IV-Foundation, Tokyo.

Jardine, R.J., Chow, F.C., Overy, R., Standing, J., 2005. ICP Design Methods for Driven Piles in Sands and Clays. Thomas Telford, London.

Kikuchi, Y., Mizutani, T., Yamashita, H., 2007. Vertical bearing capacity of large diameter steel pipe piles. In: Proceedings of International Workshop on Recent Advances of Deep Foundations, Taylor & Francis, London, pp. 711–716.

Kishida, H., 1967. The ultimate bearing capacity of pipe piles in sand. In: Proceedings of the Third Asian Regional Conference on Soil Mechanics and Foundation Engineering, Haifa, Israel, vol. 1, pp. 196–199.

Klos, J., Tejchman, A., 1981. Bearing capacity calculation for pipe piles. In: Proceedings of the 10th International Conference on Soil Mechanics and Foundation Engineering, Stockholm, Sweden, vol. 2, pp. 751–754.

Ko, J.Y., Jeong, S.S., 2015. The plugging effect of open-ended piles in sandy soil. Can. Geotech. J. 52 (5), 535–547.

Kolk, H. J., Baaijens, A. E., and Sender, M. 2005. Design criteria for pipe piles in silica sands. In: Proceedings of the International Symposium on Frontiers in Offshore Geotechnics, Taylor & Francis, London, pp. 711–716.

Kusakabe O., Matsumoto T., Sanadabata I., Kosuge S., Nishimura S., 1989. Report on questionnaire: predictions of bearing capacity and drivability of piles. In: Proceedings of the 12th International Conference on Soil Mechanics and Foundation Engineering, Rio de Janeiro, 5, pp. 2957–2963.

Lai, P., Mcvay, M., Bloomquist, D., Badri, D., 2008. Axial pile capacity of large diameter cylinder piles. In: From Research to Practice in Geotechnical Engineering, GSP 180, ASCE, pp. 366–384.

Lehane, B.M., Gavin, K.G., 2001. Base resistance of jacked pipe piles in sand. J. Geotech. Geoenviron. Eng. 127 (6), 473–480.

Lehane, B.M., Schneider, J.A., Xu, X., 2005. A review of Design Methods for Offshore Driven Piles in Siliceous Sand. The University of Western Australia, Perth, Australia UWA Rep. No. GEO 05358.

Liu, J.W., Zhang, Z.M., Yu, F., Xie, Z.Z., 2012. Case history of installing instrumented jacked open-ended piles. J. Geotech. Geoenviron. Eng. 138 (7), 810–820.

Matsumoto, T., Takei, M., 1991. Effects of soil plug on behavior of driven pipe piles. Soils Found. 31 (2), 14–34.

Murff, J. D., Raines, R. D., Randolph, M. F., 1990. Soil plug behavior of piles in sand. In: Proceedings of 22nd Offshore Technology Conference, Houston, Texas, Paper no. 6421, vol. 1, pp. 25–32.

O'Neill, M.W., Raines, R.D., 1991. Load transfer for pipe piles in highly pressured dense sand. J. Geotech. Eng. Div. ASCE 117 (8), 1208–1226.

Paik, K.H., 1994. Characteristics of Bearing Capacities for Open-ended Steel Pipe Piles Driven Into Cohesionless Soil. Korea Advanced Institute of Science and Technology, Daejeon, Korea Ph.D. Thesis.

Paik, K.H., Lee, S.R., 1993. Behavior of soil plugs in open-ended model piles driven into sands. Mar. Georesour. Geotechnol. 11, 353–373.

Paik, K.H., Salgado, R., 2003. Determination of the bearing capacity of open-ended piles in sand. J. Geotech. Geoenviron. Eng. 129 (1), 46–57.

Paik, K.H., Kim, Y.S., Lee, S.R., 1996. Effects of pile diameter on the plugging rate and bearing capacity of open-ended piles. J. Korean Geotech. Soc. 12 (2), 85–94.

Paik, K.H., Salgado, R., Lee, J.H., Kim, B.J., 2003. Behavior of open- and closed-ended piles driven into sands. J. Geotech. Geoenviron. Eng. 129 (4), 296–306.

Paikowsky, S.G., 1989. A Static Evaluation of Soil Plug Behavior with Application to the Pile Plugging Problem. Massachusetts Institute of Technology, Cambridge, MA D.Sc. Thesis.

Paikowsky, S. G., 1990. The mechanism of pile plugging in sand. In: Proceedings of the 22nd Offshore Technology Conference, Houston, TX, OTC 6490, vol. 4, pp. 593–604.

Pump W., Korista S., Scott J., 1998. Installation and load testing of deep piles in Shanghai alluvium. In: Proceedings of the Seventh International Conference on Deep Foundations, Vienna. Paper 13, pp. 131–137.

Randolph, M.F., 1988. The axial capacity of deep foundations in calcareous soil (state-of-the-art-report). In: Proceedings of International Conference Calcareous Sediments, Perth, Australia, vol. 2, pp. 837−857.

Randolph, M.F., Leong, E.C., Houlsby, G.T., 1991. One-dimensional analysis of soil plugs in pipe piles. Geotechnique 41 (4), 587–598.

Reinhall, P.G., Dahl, P.H., 2011. Underwater Mach wave radiation from impact pile driving: theory and observation. J. Acoust. Soc. Am. 130 (3), 1209–1216.

Shioi, Y., Yoshida, O., Meta, T., Homma, M., 1992. Estimation of Bearing Capacity of Steel Pipe Piles by Static Loading Test and Stress-Wave Theory, Application of Stress-Wave Theory to Piles. Balkema, Rotterdam 325–330.

Szechy, C.H., 1959. Tests with tubular piles. Acta Tech. Hung. Acad. Sci. 24, 181–219.

Thandavamoorthy, T.S., 2004. Piling in fine and medium sand-a case study of ground and pile vibration. Soils Dyn. Earthquake Eng. 24, 295–304.

Yu, F., Yang, J., 2012. Base capacity of open-ended steel pipe piles in sand. J. Geotech. Geoenviron. Eng. 138 (9), 1116–1128.